International Journal of Thermophysics, Vol. 8, No. 5, 1987

A Microsecond-Resolution Transient Technique for Measuring the Heat of Fusion of Metals: Niobium

A. Cezairliyan[1] and J. L. McClure[1]

Received January 27, 1987

A microsecond-resolution pulse-heating technique is described for the measurement of the heat of fusion of refractory metals. The method is based on rapid resistive self-heating of the specimen by a high-current pulse from a capacitor discharge system and measurement of the current through the specimen, the voltage across the specimen, and the radiance temperature of the specimen as a function of time. Melting of the specimen is manifested by a plateau in the temperature versus time function. The time integral of the power absorbed by the specimen during melting yields the heat of fusion. Measurements gave a value of 31.1 $kJ \cdot mol^{-1}$ for the heat of fusion of niobium, with an estimated maximum uncertainty of $\pm 5\%$. Electrical resistivity of solid and liquid niobium at its melting temperature was also measured.

KEY WORDS: electrical resistivity; heat of fusion; high temperatures; melting; niobium; pulse heating; refractory metals; transient techniques.

1. INTRODUCTION

Conventional methods of steady-state and quasi-steady-state measurements of thermophysical properties of refractory metals around their melting points present several serious, and sometimes unsurmountable, technical problems that result from the exposure of the specimen and its immediate environment to high temperatures for long periods. Some of the difficulties arise from chemical reactions, heat losses, evaporation, loss of mechanical strength, etc.

The problem of chemical reactions has been partially solved by the technique that utilizes electromagnetic levitation combined with drop calorimetry [1–3]. This technique makes it possible to measure enthalpies

[1] Thermophysics Division, National Bureau of Standards, Gaithersburg, Maryland 20899, U.S.A.

0195-928X/87/0900-0577$05.00/0

840/8/5-5*

of liquid as well as of solid specimens. However, this relatively slow (seconds to minutes) technique is limited in temperature because of severe radiative heat losses and high vapor pressures of liquid metals.

The above problems are reduced to a negligible level through the use of the pulse-heating techniques. These techniques are typically classified according to the duration of the experiment: subsecond (heating rates, 10^3–10^4 K · s^{-1}) and submillisecond (heating rates, 10^7–10^9 K · s^{-1}).

The subsecond pulse-heating methods, also referred to as millisecond-resolution methods, have been successfully applied to measurements of thermophysical properties of refractory metals up to their melting temperatures [4–6]. In these techniques, the melting temperature is the upper limit because the specimen, once partially molten, collapses under the gravitational force. Extension of this technique to somewhat above the melting temperature of the specimen with the objective of measuring the heat of fusion of niobium has been described previously [7]. In this case, the specimen configuration consisted of a strip of niobium between two strips of another metal (tantalum) with a higher melting temperature.

The submillisecond pulse-heating methods, also referred to as microsecond-resolution methods or capacitor-discharge methods, are particularly applicable to the measurement of properties of liquid metals [8–13]. Because of the extremely short experiment duration associated with these techniques, it is possible to have excursions of up to several thousand degrees into the liquid phase before the specimen collapses. Also, because of the short duration, interferences due to undesirable phenomena become negligibly small. However, due to additional experimental difficulties associated with higher speeds, the uncertainties in the reported results from submillisecond pulse-heating techniques are considerably higher than those from slower pulse techniques.

In this paper, a submillisecond (microsecond-resolution) pulse-heating technique is described for the accurate measurement of the heat of fusion of refractory metals and the details of measurements on niobium are given.

2. METHOD AND DESCRIPTION OF THE SYSTEM

The microsecond-resolution technique for measuring heat of fusion is based on rapid resistive self-heating of the specimen by a short-duration current pulse from a capacitor discharge system. While the specimen is heating, simultaneous measurements of current through the specimen, voltage across the specimen, and radiance temperature of the specimen are made with microsecond resolution. The heat of fusion is determined from the energy absorbed by the specimen during the melting plateau period.

A functional diagram of the microsecond-resolution system in shown in Fig. 1. The specimen (sample) is connected in series, through switch 1, to a 24-kJ capacitor bank (120 μF, 20 kV). Because of the low resistance of metal specimens (typically 1 to 50 mΩ), the discharge circuit behaves as an underdamped RLC circuit with exponentially damped oscillations at a nominal frequency of 10 kHz (upper trace in Fig. 2). The oscillatory nature of the circuit is minimized by operating it in a crowbar mode using switch 2. In crowbar operation, switch 2 is closed just after the circuit current reaches its initial peak value (about 25 μs after switch 1 is closed). This creates an electrical short across the specimen and allows the energy stored magnetically during the initial rise of the current to be returned to the circuit as unidirectional current through the specimen (lower trace in Fig. 2). Both switches are high-voltage mercury vapor ignitron tubes.

The current through the specimen is measured with current transformer PT-1, which is rated to 50 kA with a nominal sensitivity of 0.005 V/A. The output of this transformer is further reduced by a 50:1 voltage divider (not shown in the figure). The voltage across the specimen is determined by measuring the current through a high-resistance path connected in parallel across the specimen. This path has a resistance typically 1000 to 10,000

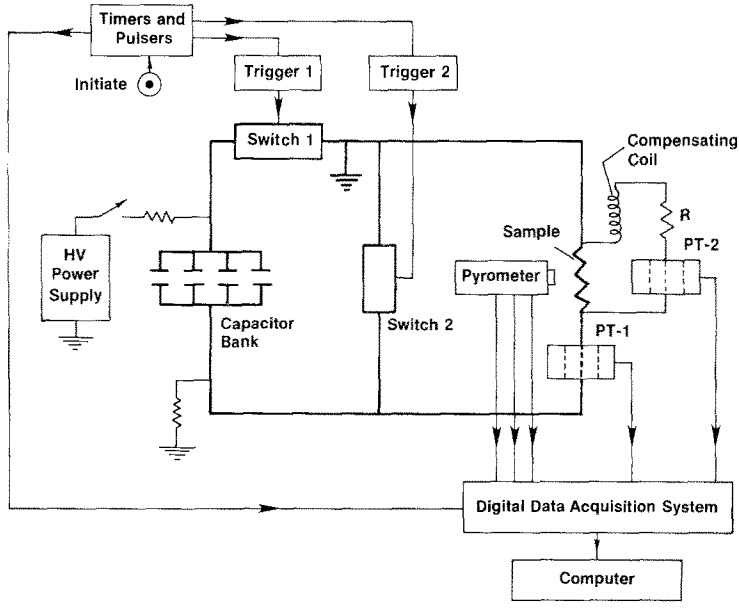

Fig. 1. Functional diagram of the microsecond-resolution system for thermophysical measurements at high temperatures.

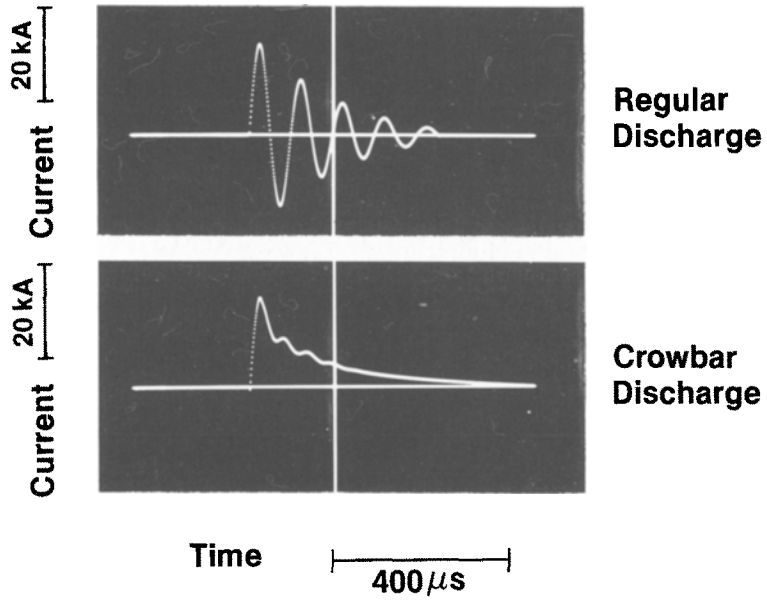

Fig. 2. Oscilloscope trace photographs of current waveforms for oscillatory (upper trace) and crowbar (lower trace) capacitor-discharge conditions.

times larger than the resistance of the specimen. In Fig. 1, the total resistance of the parallel path including lead wires and connections is represented by resistance R. The current through this path is measured with current transformer PT-2 with a nominal sensitivity of 0.02 V/A. The use of current transformers to measure electrical quantities effectively isolates the data acquisition system from high voltages at the specimen.

Inductance of the specimen and inductive coupling between the parallel path and the main circuit add inductive components to the voltage measured across the specimen. To compensate for these inductive components, a small coil in the parallel path, positioned so that it is magnetically coupled to the main circuit, is rotated until its induced voltage just cancels the original induced voltages. This compensation occurs when the two measured currents are in phase with one another. When there is no phase difference between the two measured currents, the voltage determined from the parallel path current is the resistive component of voltage across the specimen and can be used to determine absorbed energy and specimen resistance. Phase compensation is accomplished by performing a nondestructive low-voltage oscillatory discharge experiment through the specimen and examining the phase relationship between the waveforms. Details of the measurement of electrical quantities

(current and voltage) in high-voltage discharges and calibration procedures are given in another publication [14].

The radiance temperature of the specimen is measured with a special microsecond-resolution pyrometer capable of measuring the radiance temperature at two wavelengths (0.65 and 0.9 μm) in the temperature range 2000 to 6000 K. In the present work, only the 0.65-μm channel was used. The bandwidth of the channel is approximately 0.03 μm and the circular area viewed by the pyrometer is 0.5 mm in diameter. The construction and operational details of the high-speed pyrometer are given elsewhere [15].

The data acquisition system is a four-channel, digital oscilloscope with 12-bit resolution capable of recording 4096 data points per channel at a rate of 2 MHz (0.5 μs between data points). The digital oscilloscope is directly interfaced to a desktop computer for data analysis. The computer has graphics capabilities which allow immediate graphical presentation of computed results.

3. MEASUREMENTS ON NIOBIUM

Measurements were made on seven niobium specimens in the form of wires with the following nominal dimensions: diameter, 1.6 mm; and length, 63.5 mm. The specimen was clamped into a specimen chamber as illustrated in Fig. 3. Voltage probes, made of niobium strips (6.4 mm wide and 0.13 mm thick), were placed on knife marks about 25 mm apart made on the middle portion of the specimen. The ends of the strips in contact with the specimen were sharpened to a knife edge. The voltage probes were given a "C-shaped" bend to provide flexibility and constant pressure against the specimen. The knife marks defined an "effective" specimen free of axial temperature gradients for the duration of the experiment. The distance between the knife-edge marks on the specimen was measured using a traveling microscope. After inserting the specimen chamber into the discharge circuit, the parallel circuit was soldered to the knife edges using the solder lugs.

The linear density of the niobium wire was measured to be $0.1690\ \mathrm{g \cdot cm^{-1}}$. As reported by the manufacturer, the niobium material was 99.9+ % pure. The total amount of impurities in the material was reported to be less than 613 ppm. The impurity list is as follows: Ta, 100 ppm; 0, 73 ppm; W, 50 ppm; N, 29 ppm; Zr, Mo, Ti, Fe, Ni, Si, Mn, Ca, Al, Cu, Sn, Cr, V, Co, Mg, Pb, and Hf, each less than 20 ppm; and C, H, B, and Cd, together less than 21 ppm.

Prior to the experiments, each specimen was subjected to four heating pulses (about 1 s long) from a battery bank to remove oxides from the surface. Each of these pulses heated the specimen to a radiance temperature of

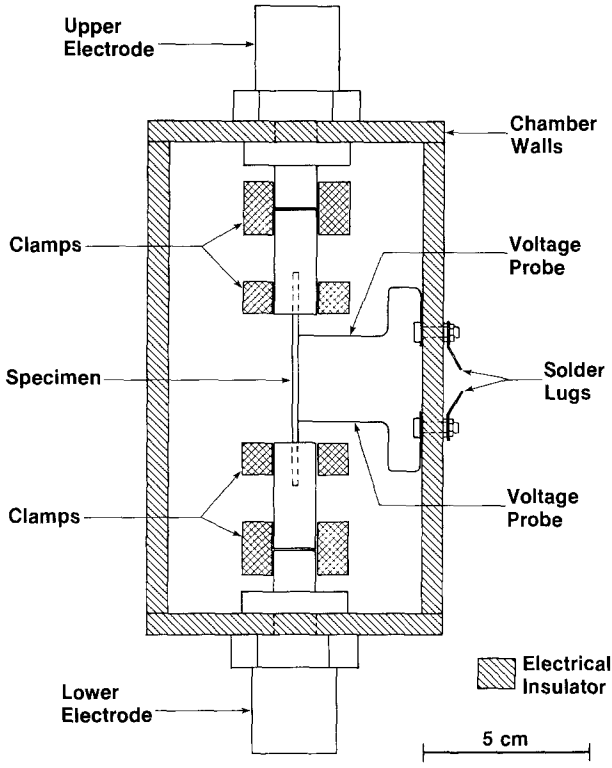

Fig. 3. Schematic diagram of the specimen chamber showing the arrangement of the specimen, clamps, and voltage probes.

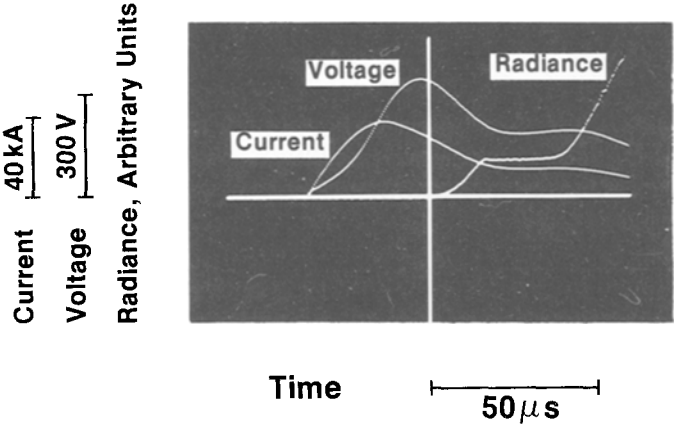

Fig. 4. Oscilloscope trace photograph showing the current, voltage, and radiance waveforms during a typical experiment.

about 2000 K. Before each experiment, the total resistance of the parallel path including the specimen and knife-edge contacts was measured with a high-precision digital multimeter. The resistance of this path was either 20.08 or 20.09 Ω for each of the seven experiments. Each experiment was conducted with the specimen in an argon environment at slightly above atmospheric pressure.

The pyrometer was calibrated using a tungsten filament reference lamp, which has been calibrated against the National Bureau of Standards Photoelectric Pyrometer by the Radiometric Physics Division at the NBS. All reported temperatures are based on the International Practical Temperature Scale of 1968 [16]. Pyrometer calibration performed before and after the series of the pulse experiments did not indicate any significant difference.

In a typical experiment, the capacitor bank was charged to an initial voltage of about 6.7 kV and discharged in the crowbar mode of operation. The specimen was heated from room temperature through the melting temperature to a radiance temperature of about 2800 K in approximately 100 μs. An oscilloscope trace photograph showing the time variation of current, voltage, and specimen radiance for a typical experiment is shown in Fig. 4. The trace with the higher peak is the voltage and the trace with the lower peak is the current. The apparent phase difference between the two traces is most likely due to the rapidly increasing resistance of the specimen as it heats. The peak voltage across the specimen was typically 350 V, and the peak current through the specimen was typically between 40 and 45 kA. The plateau in the radiance trace indicates the melting of the specimen. The liquid specimen continues to heat for approximately another 400 K above the melting temperature. The heating rate in the solid phase is about $5 \times 10^7\ \mathrm{K \cdot s^{-1}}$ at a temperature approximately 200 K below the plateau and the heating rate in the liquid phase is about $2 \times 10^7\ \mathrm{K \cdot s^{-1}}$ at a temperature approximately 200 K above the plateau.

For each experiment, it was important to know that the voltage probes did not move away from the knife marks on the specimen. This was checked by using the current and voltage data to compute the specimen resistance as a function of time and displaying the results graphically. Any motion of the probes would show up as a sudden change in the resistance curve. The variation of resistance as a function of time for a typical experiment is shown in Fig. 5. The resistance of the effective specimen increased from about 2.5 to about 14 mΩ during a typical experiment. The resistance of the specimen was almost constant in the liquid phase. For comparison purposes, the radiance temperature of the specimen as a function of time is also displayed in Fig. 5.

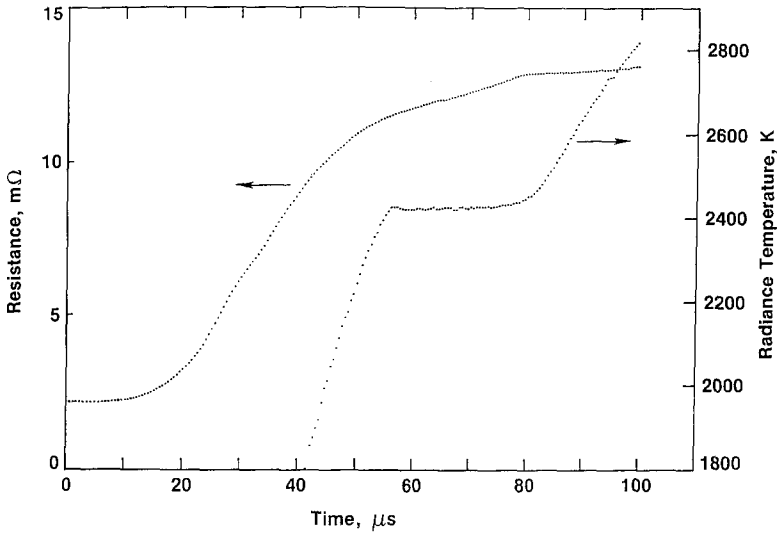

Fig. 5. Variation of resistance (obtained from each individual measurement of current and voltage) and radiance temperature of the specimen as a function of time during premelting, melting (plateau), and postmelting periods for a typical experiment.

4. RESULTS

The heat of fusion of a niobium specimen was determined from the energy absorbed by the specimen during the melting period. The procedure is as follows. From the measured data for current and voltage, the absorbed power for each individual point was computed as illustrated in Fig. 6. The energy absorbed by the specimen above an arbitrary temperature (2000 K) was detemined by integrating power point by point over time to a radiance temperature of about 2800 K. The mass of the "effective" specimen was determined from the measurements of total mass, total length, and "effective" length. A value of 92.91 for the atomic weight of niobium was used to express absorbed energy in units of $J \cdot mol^{-1}$. Because of the speed of the experiments, no correction for heat losses due to thermal radiation or conduction was required. The result for a typical experiment is illustrated in Fig. 7, which shows the relationship of radiance temperature as a function of absorbed energy.

The radiance temperature data as illustrated in Fig. 7 were fitted, by the least-squares method, to a quadratic function for the premelting region and linear functions for the melting (plateau) region and the postmelting region. The standard deviation of the fits in each region ranged between the

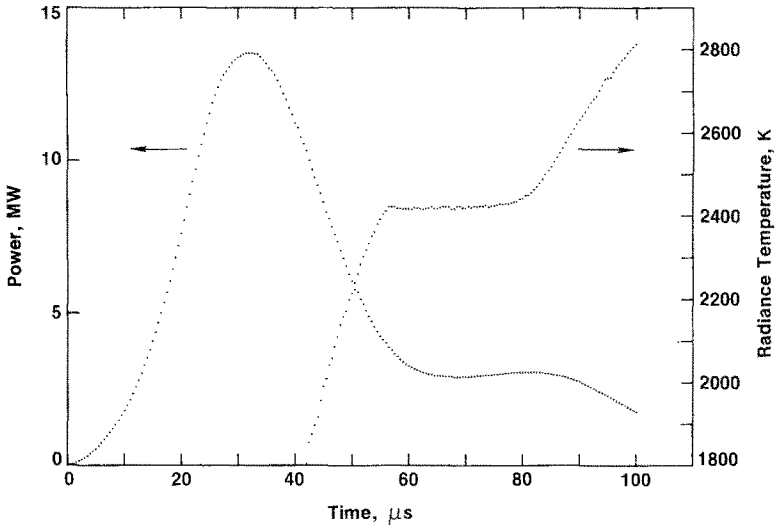

Fig. 6. Absorbed power (obtained from each individual measurement of current and voltage) and radiance temperature of the specimen during premelting, melting (plateau), and postmelting periods for a typical experiment.

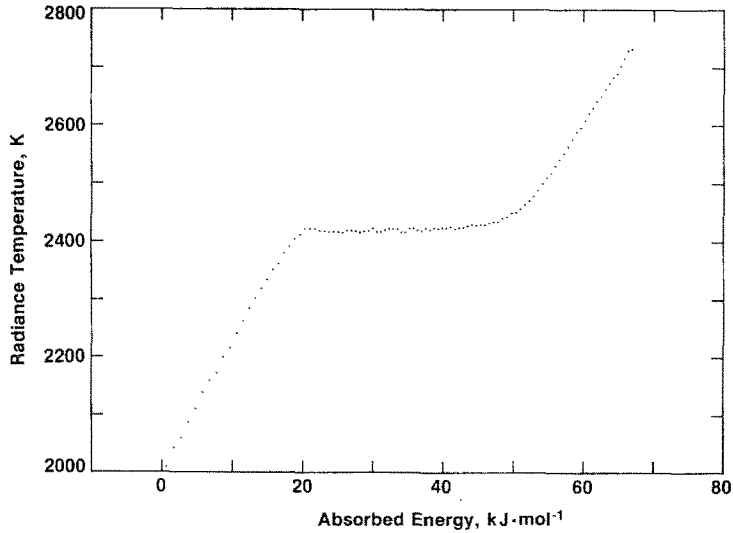

Fig. 7. Variation of radiance temperature as a function of absorbed energy by the specimen above 2000 K obtained by integrating power point by point over time during premelting, melting (plateau), and postmelting periods for a typical experiment.

Table I. Experimental Results on the Heat of Fusion of Niobium

Specimen No.	Heating time to start of melting (μs)	Radiance temperature at start of melting (K)	Duration of melting plateau (μs)	Slope of melting plateau ($K \cdot \mu s^{-1}$)	Heat of fusion ($kJ \cdot mol^{-1}$)
1	50.8	2408.7	24.5	0.820	31.3
2	52.7	2414.4	25.3	0.455	31.1
3	48.8	2408.6	25.3	0.518	31.1
4	51.6	2413.3	26.8	0.597	30.5
5	49.2	2411.5	25.8	0.457	30.8
6	52.6	2410.5	30.8	0.418	31.6
7	49.2	2415.3	25.9	0.518	31.2

minimum and the maximum values that follow: premelting region, 3.2–5.0 K; plateau region, 1.4–2.1 K; and postmelting region, 0.9–1.6 K. The beginning and end of the melting plateau were defined by the intersections of the temperature versus absorbed energy curves for each region. The heat of fusion for each experiment was obtained from the difference between the value of the absorbed energy at the end of the melting plateau and the value of the absorbed energy at the beginning of the melting plateau. The experimental results for heat of fusion of niobium are given in Table I. The average of these values is $31.1\ kJ \cdot mol^{-1}$, with an average deviation of $0.3\ kJ \cdot mol^{-1}$ and a maximum absolute deviation of $0.6\ kJ \cdot mol^{-1}$.

Using room-temperature dimensions, the electrical resistivity of solid niobium (ρ_s) and of liquid niobium (ρ_l) at the melting temperature was determined from the resistance of the specimen at the two intersection points used to obtain the heat of fusion. The experimental results for electrical resistivity of niobium are given in Table II. The averages of these

Table II. Experimental Results on the Electrical Resistivity of Solid (ρ_s) and Liquid (ρ_l) Niobium at Its Melting Temperature

Specimen No.	ρ_s ($\mu\Omega \cdot cm$)	ρ_l ($\mu\Omega \cdot cm$)	ρ_l/ρ_s
1	89.8	100.6	1.120
2	89.7	100.8	1.124
3	90.0	100.5	1.116
4	90.7	100.9	1.112
5	89.9	100.4	1.117
6	90.5	100.8	1.114
7	90.2	100.5	1.114

values are 90.1 $\mu\Omega \cdot$ cm for solid and 100.6 $\mu\Omega \cdot$ cm for liquid niobium at its melting temperature. The mean value of the resistivity ratio, ρ_l/ρ_s, is 1.117, with an average absolute deviation of 0.004 and a maximum absolute deviation of 0.007.

5. ESTIMATE OF ERRORS

The sources of error that contribute to the uncertainty (total systematic and random errors) in the reported values of heat of fusion and electrical resistivity are discussed below.

5.1. Electrical Measurements

Estimates of errors in electrical quantities, current and voltage, measured with the present system have been discussed in detail elsewhere [14]. It has been shown that each quantity can be measured with a maximum uncertainty of $\pm 1\%$.

5.2. Temperature Measurements

Estimates of errors in temperature measurements with the microsecond-resolution pyrometer have been discussed at length in an earlier publication [15]. The results indicate that the radiance temperature at 0.65 μm can be measured with an uncertainty not exceeding ± 4 K at 2500 K, which is about the middle of the temperature region in this investigation. Since in the present work data on radiance temperature are used only to identify the beginning and end of the melting period, absolute errors in temperature measurements do not have any significant effect on the reported properties. However, imprecision (reproducibility) of temperature measurements which is better than ± 1 K is significant, since it affects the reliability of the curve fitted through the temperature data.

5.3. Melting Duration

The maximum uncertainty in determining the duration of the melting period in the present experiments is estimated to be about ± 1 μs. This corresponds to an uncertainty in the heat of fusion value of approximately $\pm 4\%$. This value reflects uncertainties that arise from the imprecision of the temperature data and from the forms of the mathematical functions and ranges used in fitting the temperature data during the premelting, melting, and postmelting periods.

5.4. Mass of the Specimen

The quantities that affect the determination of the mass of the effective specimen are the linear density of the niobium wire and the distance between the voltage probe marks. The linear density was obtained by weighing the entire specimen and dividing it by the total length. Mass measurements were performed with an uncertainty of $\pm 0.01\%$. Length measurements were made with an uncertainty of $\pm 0.1\%$. The finite thickness of the voltage probes and their positioning on the specimen can create a significant additional uncertainty in the effective length of the specimen, which may be as high as $\pm 1\%$. Therefore, the uncertainty in determining the mass of the specimen is about $\pm 1\%$.

5.5. Temperature Distribution in the Specimen

Uniformity of the temperature distribution in the specimen, at any given time during heating, may be affected either by heat transfer processes or by nonuniform heating. Heat transfers by conduction, convection, and even radiation in the present experiments are relatively slow processes and do not contribute to the establishment of temperature gradients in the effective specimen. The major source of temperature nonuniformities in the specimen during rapid pulse heating is likely to be the hot spots or zones that result from material inhomogeneities or geometrical nonuniformities in the specimen. Special effort has been made to select specimens with a high degree of cross-sectional uniformity. It is difficult to quantify this, and since its effect is likely to be random, the ultimate check is the reproducibility of the measured property. The skin effect which is caused by changing currents in a circuit alters the resistance (in the radial direction) of the specimen and, thus, creates temperature nonuniformities in the specimen. The magnitude of the skin effect depends on the frequency of the current, the electrical resistivity of the specimen material, and the diameter of the specimen. For the specimens and operational conditions of the present work, the contribution of the skin effect to the measured energy is estimated to be about 0.07% near the room temperature and becomes even smaller near the melting temperature because of the increased resistivity of niobium with temperature.

5.6. Heat Loss from the Specimen

At the temperatures and speeds involved in the present work, the only significant heat loss from the specimen is that due to thermal radiation. For the present conditions, energy loss from the effective specimen due to

thermal radiation is much less than 0.01% of the imparted energy, thus it is completely negligible.

5.7. Summary of Errors

Uncertainty in the determination of the melting duration (4%) is by far the single largest contributor to the uncertainty in the value of the heat of fusion. Uncertainties in the other quantities, current, voltage, temperature, mass, etc., are 1% or less each. Uncertainties (random plus systematic) in the properties are obtained by taking the square root of the sum of the squares of the individual uncertainties of the relevant quantities. As a result, uncertainty from all sources in our reported value of the heat of fusion of niobium is $\pm 5\%$; similarly that of electrical resistivity is $\pm 2\%$.

6. DISCUSSION

Measurements of the heat of fusion of niobium reported in the literature (Table III) were carried out by means of either levitation calorimetry [1, 3, 17] or microsecond-resolution capacitor discharge techniques [9, 12, 18, 19], except for the earlier work in this laboratory using the millisecond-resolution technique [7]. The values reported in the literature fall into two groups: those between 30.5 and 33.1 $kJ \cdot mol^{-1}$ and those around 28 $kJ \cdot mol^{-1}$. The disagreement between these two groups of values, about 20%, does not correlate with measurement technique, since

Table III. Heat of Fusion of Niobium Reported in the Literature

Investigator	Ref. No.	Year	Heat of fusion ($kJ \cdot mol^{-1}$)	Technique
Margrave	23	1970	33.1	Levitation calorimetry
Sheindlin et al.	17	1972	27.6	Levitation calorimetry
Savvatimskii	18	1973	27.6	Pulse heating[a]
Martynyuk et al.	9	1975	33.0	Pulse heating[a]
Shaner et al.	19	1977	27.9	Pulse heating[a]
Cezairliyan and Miiller	7	1980	31.5	Pulse heating[b]
Betz and Frohberg	3	1980	30.5	Levitation calorimetry
Gallob et al.	12	1985	28.7	Pulse heating[a]
Present work			31.1	Pulse heating[a]

[a] Capacitor-discharge technique yielding melting times in the range of about 10^{-4} to 10^{-6} s.
[b] Energy supplied by a battery bank yielding melting times in the range of about 10^{-1} to 10^{-2} s.

values obtained using a given technique can be found in either group. The values in the group between 30.5 and 33.1 $kJ \cdot mol^{-1}$ are within 6.5% of the value reported here. This difference lies within the combined experimental uncertainties. The reported values in the other group are all about 10% lower than the present result except that of Gallob et al. [12], which is about 8% lower than the present value. It is of interest to note that the value obtained earlier in this laboratory by Cezairliyan and Miiller [7], using a much slower millisecond technique, is only 1.3% higher than the value reported here.

Using the value of 31.1 $kJ \cdot mol^{-1}$ for the heat of fusion of niobium and 2750 K for the melting temperature of niobium [20], a value of 11.3 $J \cdot mol^{-1} \cdot K^{-1}$ for the entropy of fusion of niobium is obtained. This experimental value is considerably higher than the value of 7.4 $J \cdot mol^{-1} \cdot K^{-1}$ suggested by Gschneidner [21] for body-centered cubic metals.

The radiance temperature of the specimen during the melting period of each experiment (Fig. 7) shows a small positive slope, a behavior typically observed in capacitor discharge experiments. Shaner et al. [19] have suggested that this occurs as a result of a change in the apparent emissivity of the metal or as a result of nonequilibrium melting. The latter explanation may also be the reason for the lack of a sharp discontinuity in the heating curve at the end of the melting period. Due to the speed of the experiments, it is possible that small regions that have completely melted

Table IV. Electrical Resistivity[a] of Solid (ρ_s) and Liquid (ρ_l) Niobium at Its Melting Temperature as Reported in the Literature

Investigator	Ref. No.	Year	Resistivity at the melting temp. ($\mu\Omega \cdot cm$)		Resistivity ratio, ρ_l/ρ_s
			ρ_s	ρ_l	
Savvatimskii	18	1973	95.2	108.5	1.14
Martynyuk et al.	9	1975	86.9	102.7	1.18
Shaner et al.	19	1977	89[b]	101[b]	1.13
Cezairliyan and Miiller	7	1980	89.8	100.5	1.12
Gallob et al.	12	1985	87.6	97.1	1.11
Present work			90.1	100.6	1.12

[a] All data except for those of Ref. 19 are based on room-temperature dimensions of the specimen.

[b] Corresponding values based on room-temperature dimensions are $\rho_s = 87$ and $\rho_l = 98$.

will continue to heat while nearby regions are still melting. Such a non-equilibrium behavior would give rise to a positive slope in the specimen radiance temperature during the melting period.

Table IV shows that the results of electrical resistivity change of niobium at the melting temperature as reported here are in good agreement with the previous value reported by this laboratory. All the other reported results were obtained from capacitor-discharge techniques.

In conclusion, the experimental results on niobium have demonstrated the ability of the microsecond-resolution system to provide accurate values of the heat of fusion of electrically conducting refractory substances.

ACKNOWLEDGMENTS

This work was supported in part by the Microgravity Science and Applications Division of NASA. The assistance of M. S. Morse and G. M. Foley in connection with electronic and optical instrumentation is greatly appreciated.

REFERENCES

1. V. Ya. Chekhovskoi, A. E. Sheindlin, and B. Ya. Berezin, *High Temp. High Press.* **2**:301 (1970).
2. A. K. Chaudhuri, D. W. Bonnell, L. A. Ford, and J. L. Margrave, *High Temp. Sci.* **2**:203 (1970).
3. G. Betz and M. G. Frohberg, *Z. Metallkde.* **71**:451 (1980).
4. A. Cezairliyan, M. S. Morse, H. A. Berman, and C. W. Beckett, *J. Res. Natl. Bur. Stand. (USA)* **74A**:65 (1970).
5. A. Cezairliyan, *J. Res. Natl. Bur. Stand. (USA)* **75C**:7 (1971).
6. A. Cezairliyan, *Int. J. Thermophys.* **5**:177 (1984).
7. A. Cezairliyan and A. P. Miiller, *Int. J. Thermophys.* **1**:195 (1980).
8. I. Ya. Dikhter and S. V. Lebedev, *High Temp. High Press.* **2**:55 (1970).
9. M. M. Martynyuk, I. Karimkhodzhaev, and V. I. Tsapkov, *Sov. Phys. Tech. Phys.* **19**:1458 (1975).
10. G. R. Gathers, J. W. Shaner, and R. L. Brier, *Rev. Sci. Instrum.* **47**:471 (1976).
11. U. Seydel, H. Bauhof, W. Fucke, and H. Wadle, *High Temp. High Press.* **11**:35 (1979).
12. R. Gallob, H. Jager, and G. Pottlacher, *High Temp. High Press.* **17**:207 (1985).
13. A. Berthault, L. Arles, and J. Matricon, *Int. J. Thermophys.* **7**:167 (1986).
14. A. Cezairliyan and J. L. McClure, In preparation.
15. G. M. Foley, M. S. Morse, and A. Cezairliyan, in *Temperature: Its Measurement and Control in Science and Industry, Vol. 5*, J. F. Schooley, ed. (Am. Inst. Phys., New York, 1982), p. 447.
16. International Practical Temperature Scale of 1968. *Metrologia* **5**:35 (1969).
17. A. E. Sheindlin, B. Ya. Berezin, and V. Ya. Chekhovskoi, *High Temp. High Press.* **4**:611 (1972).
18. A. I. Savvatimskii, *High Temp. (USSR)* **11**:1057 (1973).

19. J. W. Shaner, G. R. Gathers, and W. M. Hogson, in *Proceedings of the Seventh Symposium on Thermophysical Properties*, A. Cezairliyan, ed. (ASME, New York, 1977), p. 896.
20. A. Cezairliyan, *High Temp. High Press.* **4**:453 (1972).
21. K. A. Gschneidner, in *Solid State Physics, Vol. 16*, F. Seitz and D. Turnbull, eds. (Academic, New York, 1965), p. 275.
22. A. Cezairliyan, *J. Res. Natl. Bur. Stand. (USA)* **77A**:333 (1973).
23. J. L. Margrave, *High Temp. High Press.* **2**:583 (1970).